Journal of Physics: Conference Series **2531** (2023) 012001 doi:10.1088/1742-6596/2531/1/012001

Superconductors in strong electric fields: Quantum Electrodynamics meets Superconductivity

Andrea Amoretti

Dipartimento di Fisica, Università di Genova, via Dodecaneso 33, I-16146, Genova, Italy
&
I.N.F.N. - Sezione di Genova, via Dodecaneso 33, I-16146, Genova, Italy

E-mail: andrea.amoretti@ge.infn.it

Abstract. A static electric field has always been thought to play little role in the physics of ideal conductors, since the screening effects of mobile carriers prevent it from penetrating deep into the bulk of a metal. Very recently however, experimental evidence has been obtained which indicates that static electric fields can be used to manipulate the superconductive properties of metallic BCS superconducting thin films, weakening the critical current. In this paper I will show how possible explanations to this striking effect can be found relying on the analogy between Superconductivity and Quantum Electrodynamics noticed by Nambu and Iona-Lasinio in the sixties. I will show that, following this parallelism, it is possible to predict a new phenomenon: the superconducting Schwinger effect. Secondly I will explain how this new microscopic effect can be connected to a modified Gizburg-Landau theory where additional couplings between electric field and the superconductive condensate are taken into account. Eventually I will connect these theoretical predictions to the experiments, proposing them as a possible explanation of the weakening of superconductivity due to an external electric field.

1. Introduction

There is no electrostatic field in the bulk of an ideal conductor. The screening of the electric field occurs due to the presence of mobile charge carriers which, under the external electric field, redistribute themselves inside the conductor and generate an excess of the electric charge density at its boundary. The redistributed charges create their own electric field which compensates for the external field inside the conductor [1]. The static electric field falls off with an exponential law, $E(x) \sim E(0)e^{-x/\lambda}$, as one moves from the conductor boundary at $x = 0$ towards its bulk, $x > 0$. The screening length λ determines the width of a layer of the redistributed mobile charges near the boundary. At high enough temperature T the charge carriers form a classical thermal plasma characterized by the Debye screening length $\lambda_{\rm D}$. At low temperature, the system enters the quantum regime of a non-relativistic Fermi gas characterized by the Thomas-Fermi screening length $\lambda_{\rm TF}$ (typically of the order of few Å), which is produced by density (rather than thermal) effects.

The situation changes in a class of materials discovered in the last decade, whose low energy properties are not described by the Fermi liquid theory but by mass-less relativistic fermions instead. Renowned members of this class of materials are graphene [2] and Dirac and Weyl semimetals [3]. In these systems the screening picture described above is not valid. On the contrary, the properties of these systems are well described by mass-less Quantum

Electrodynamics (QED) and, as in QED, the photon polarization function that encodes the screening properties acquires a logarithmic dependence on the renormalization scale [4, 5], making the effects of a static electric field inside these materials considerably more relevant. Due to this fact, these materials have been proposed as test-beds to verify QED predictions never measured such as Quantum Anomalies [6] and the Schwinger effect [7].

More surprisingly, and very recently [8], a sufficiently strong static electric field has been demonstrated to be relevant even in systems where it was always thought to play no role, namely Bardeen-Cooper-Schrieffer (BCS) superconductors [9, 10, 11, 12, 13, 14]. In [8] the authors reported field-effect control of the supercurrent in all-metallic transistors made of different BCS superconducting thin films. They found that, at low temperature, the field-effect transistors presented a monotonic decay of the critical current under increasing electrostatic field. This phenomenon is known as the Superconductive Field Effect (SFE) and the results have been recently confirmed by other experimental groups [15, 16, 17, 18, 19, 20, 21, 22].

The microscopic origin of this phenomenon is unclear. All the materials [8, 16, 15, 17, 18, 19, 20, 21, 23] analyzed are well described by the conventional BCS theory and metallic in the normal phase (hence it is surprising that the electrostatic field could play any role). It has been suggested that energetic quasi-particle injection from the gate control [16, 17] or energy or phase fluctuations [19] could be responsible for the observations. These ideas seem to be precluded by recent ionic-gating experiments, where the electric field is generated by crystallized charges [24], as there is no moving charge.

Several microscopic proposals have been suggested to explain the experimental results of [8, 16, 15, 17, 18, 19, 20, 21]. These include electric-field induced spin-orbit polarization [25], Rashba-like surface effects [26]. All these proposals lead to a weakening of superconductivity but they do not fully explain other experimental results [8, 24, 27, 28, 29, 30, 31, 32] .

Given that the SFE persists in many different compounds with different experimental setups and geometries [27, 28, 33, 34, 35, 36, 37], in [38, 39] we suggested that the phenomenon is a property of including the electric field in standard BCS theories. More precisely, in [38] we demonstrated how the inclusion of a constant electric field into the BCS equations can lead to the creation of Schwinger-like excitations which can destroy the superconductive condensate due to decoherence of the ground state. Even though the result in [38] are promising, screening effect of the electric field are not included, and consequently the model is valid only in a thin portion of the sample near the boundary, where the electric field completely penetrates. To overcome this issue, in [39] we followed an effective field theory approach, considering the effect of additional electric field dependent terms in a Ginzburg-Landau model, and treating the electric field as a non-dynamical field, with a fixed exponentially decaying profile. This phenomenological approach allowed us to prove that, even considering screening effect, there is room for the electric field to cause a phase transition of the superconductor to the normal metal phase.

The aim of this paper is to review the results of [38, 39] and to propose possible future developments to join the microscopical analysis of [38] with the effective field theory description of [39], which can lead to a complete theoretical understanding of the SFE.

2. The superconductive Sauter-Schwinger effect: decoherence at the boundary

One of the most remarkable predictions of QED is spontaneous particle production from the vacuum in the presence of a strong electromagnetic field (for reviews, see Refs. [40, 41, 42]). This surprising effect was first discovered by Sauter in 1931 [43]. Sauter's idea was expanded later by Heisenberg and Euler [44] and by Schwinger [45], who fully formulated the idea within quantum field theory for the first time. Thus, the vacuum particle production by a strong electromagnetic field is called the Schwinger mechanism. It is essentially an electric effect. In the presence of a strong electric field, there occurs a level crossing between the Dirac sea and the positive energy continuum. Then, an electron filling the Dirac sea can tunnel into the positive energy continuum,

leaving a hole in the Dirac sea. An electron/positron pair is spontaneously produced, which can be understood as the QED analogue of electrical breakdown or the Landau-Zener transition in materials [46, 47, 48].

In [38] I proposed that an analogous mechanism can occur in superconductors. My proposal relies on formalizing and extending a striking similarity between the Dirac equation and the Bogoliubov-de Gennes equations describing the elementary excitations of a superconductor [49, 50, 51, 52], noticed by Nambu and Jona-Lasinio in the Sixties. In fact, if one looks at the two equations,

Dirac equations	**Bogoliuvov-de Gennes equations**
$E\psi_L = \boldsymbol{\sigma}\cdot\boldsymbol{k}\psi_L + m\psi_R$	$E_{\boldsymbol{k}}u^*_{\boldsymbol{k}} = (\epsilon_{\boldsymbol{k}}-\mu)\,u^*_{\boldsymbol{k}} + \Delta_{\boldsymbol{k}}v^*_{\boldsymbol{k}}$
$E\psi_R = -\boldsymbol{\sigma}\cdot\boldsymbol{k}\psi_R + m\psi_L$	$E_{\boldsymbol{k}}v^*_{\boldsymbol{k}} = -(\epsilon_{\boldsymbol{k}}-\mu)\,v^*_{\boldsymbol{k}} + \Delta_{\boldsymbol{k}}u^*_{\boldsymbol{k}}$

it is easy to notice that they are formally identical if one identifies the Dirac particle with a quasi-particle excitation in the superconductor and the fermion mass with the superconducting energy gap [51], namely

$$\begin{gathered}\psi_L \leftrightarrow u^*_{\boldsymbol{k}}\\ \psi_R \leftrightarrow v^*_{\boldsymbol{k}}\\ \boldsymbol{\sigma}\cdot\boldsymbol{k} \leftrightarrow (\epsilon_{\boldsymbol{k}}-\mu)\\ m \leftrightarrow \Delta\\ \text{vacuum} \leftrightarrow \text{Condensate}\end{gathered}$$

This makes the dynamics of superconductors very similar to massive QED. In the spirit of the superconductor-QED analogy [49, 50, 51, 52], in [38], I proposed that superconductors must present the same kind of vacuum instability, generating a phenomenon analogous to the Schwinger effect, the *Superconductive Schwinger effect* (SSE).

In the Dirac vacuum the enormous electric field required to generate the Schwinger vacuum instability is determined by the electron mass $m_e = 0.5$ MeV$/c^2$ and the electron charge e [41],

$$E_{\rm c}^{\rm QED} = \frac{m_e^2c^3}{\hbar e} \sim 10^{18}\frac{V}{m}\ ,$$

making the QED Schwinger effect impossible to detect in a laboratory. However, if we replace m_ec^2 with the superconducting gap Δ ($\sim$100 μeV $-$ 1 meV for conventional superconductors), we drastically reduce the critical electric field:

$$E_{\rm c}^{\rm SSE} = \frac{\Delta^2}{\hbar ce} \sim 10^{8}\frac{V}{m}\ .$$

$E_{\rm c}^{\rm SSE}$ is an electrostatic field which, contrary to $E_{\rm c}^{\rm QED}$, can be achieved in modern laboratories. Most importantly, it is of the same order of magnitude of the one needed in [8] to suppress the critical current. In the following sections, I will review how this effect can be seen to emerge from the BCS equations and I will argue that the SSE can be the microscopic origin of the phenomenon measured in [8].

2.1. General framework

To derive the dynamics of a superconductor immersed in an external electric field we start from the usual effective BCS Hamiltonian [10]:

$$H_{eff} = \int d\mathbf{r}\ \Big\{\ \sum_{\alpha}\Big[\Psi^\dagger(\alpha\mathbf{r})H_e(\mathbf{r})\Psi(\alpha\mathbf{r}) + \Delta(\mathbf{r})\Psi^\dagger(\mathbf{r}\uparrow)\Psi^\dagger(\mathbf{r}\downarrow) + \Delta^*(\mathbf{r})\Psi(\mathbf{r}\downarrow)\Psi(\mathbf{r}\uparrow)\Big\}\ , \tag{1}$$

where α is the spin index, Ψ is the usual fermionic field and V is the BCS coupling energy [10].

The superconductive gap is defined as:

$$\Delta(\mathbf{r}) \;=\; -V\langle\Psi(\mathbf{r}\downarrow)\Psi(\mathbf{r}\uparrow)\rangle = V\langle\Psi(\mathbf{r}\uparrow)\Psi(\mathbf{r}\downarrow)\rangle \;, \tag{2}$$

and has to be computed self-consistently from the BCS equations.

We take $H_e(\mathbf{r})$ to be the single particle Hamiltonian:

$$H_e(\mathbf{r}) = \frac{1}{2m}\Big(-i\hbar\nabla - \frac{e}{c}\mathbf{A}\Big)^2 + U_0(\mathbf{r}) - \mu \;. \tag{3}$$

In the previous equation, μ is the chemical potential which set the groundstate energy of the single particle excitations, $\mathbf{A}$ is the electromagnetic vector potential and $U_0(\mathbf{r})$ is a scalar potential, which we assume to be independent on the particle spin.

We assume the electric field to penetrate completely into the superconductor. This crucial assumption implies that, considering a bulk superconductor, the validity of the model is restricted to a thin portion of the sample near the boundary. possible generalizations and extensions of this model will be described in section 3 and section 4. Without loss of generality we consider an external electric field E_f applied along the z direction; i.e., the electric field vector is $\mathbf{E}_f = \{0, 0, E_f\}$. Eventually, we make a gauge choice such that $\mathbf{A} = 0$ and $U_0(\mathbf{r}) = eE_f z$.

Considering the usual modes decomposition of the fermionic fields in (1),

$$\begin{aligned}\Psi(\mathbf{r}\alpha) &= \sum_{\mathbf{k}} e^{i\mathbf{k}\cdot\mathbf{r}} a_{\mathbf{k}\alpha} \\ \Psi^\dagger(\mathbf{r}\alpha) &= \sum_{k} e^{-i\mathbf{k}\cdot\mathbf{r}} a^\dagger_{\mathbf{k}\alpha} \;,\end{aligned} \tag{4}$$

the effective Hamiltonian reads:

$$H_{eff} \;=\; \sum_{\mathbf{k}} \Big\{ h_{\mathbf{k}_-}(t)(a^\dagger_{\mathbf{k}\uparrow}a_{\mathbf{k}\uparrow} + a^\dagger_{\mathbf{k}\downarrow}a_{\mathbf{k}\downarrow}) - \Delta a^\dagger_{\mathbf{k}\uparrow}a^\dagger_{-\mathbf{k}\downarrow} - \Delta^* a_{\mathbf{k}\uparrow}a_{-\mathbf{k}\downarrow} \Big\} \tag{5}$$

where we have put $k_\perp^2 = k_x^2 + k_y^2$ and $\Delta = V\sum_{\mathbf{k}}\langle a_{\mathbf{k}\uparrow}a_{-\mathbf{k}\downarrow}\rangle$.

It is convenient to simplify the notation but, at the same time, keep track of the presence of the vector potential $\mathbf{A}$. For this reason, we introduce the kinetic energy $h_{\mathbf{k}_-}(t) = h_{\mathbf{k}-\frac{e}{\hbar c}\mathbf{A}}(t) = \frac{1}{2m}\Big[\hbar^2 k_\perp^2 + (\hbar k_z + eE_f t)^2\Big] - \mu$.

In the sum in Eq. (5) both positive and negative $\mathbf{k}$ contributions are present. We can separate the negative terms like $h_{-\mathbf{k}_-}a^\dagger_{-\mathbf{k}\uparrow}a_{-\mathbf{k}\uparrow}$. We have

$$h_{-\mathbf{k}_-} = h_{-\mathbf{k}-\frac{e}{\hbar c}\mathbf{A}}(t) = \frac{1}{2m}\Big[\hbar^2 k_\perp^2 + (\hbar k_z - eE_f t)^2\Big] - \mu = h_{\mathbf{k}_+} \tag{6}$$

Thus, formally reversing the momentum is equivalent to change the charge to the particle.

The superconductor pair potential can be written as $\Delta = |\Delta|e^{i\chi}$ where χ is the superconduting phase. It is related to the gauge-invariant scalar ϕ and vector $\mathbf{A}$ potentials by the equations [13]

$$\begin{aligned}\mathbf{A} &= \mathcal{A} - \frac{\hbar c}{2e}\nabla\chi \\ \phi &= \mathcal{V} + \frac{\hbar}{2e}\frac{\partial\chi}{\partial t}.\end{aligned} \tag{7}$$

These are related to the physical electric $\mathbf{E}$ and magnetic field $\mathbf{h}$ by the relations [13]

$$\begin{aligned} \mathbf{E} &= -\frac{1}{c}\frac{\partial \mathcal{A}}{\partial t} - \nabla \mathcal{V} \\ \mathbf{h} &= \nabla \times \mathcal{A}. \end{aligned} \tag{8}$$

By setting $\phi = 0$ and $\mathcal{A} = 0$, i.e., no magnetic field, we obtain

$$\chi = \frac{2e}{\hbar} E_f \; t \; z \tag{9}$$

and $\mathbf{A} = \{0, 0, -cE_f t\}$ as above. Therefore, the superconducting phase, the pairing potential (2) and the Hamiltonian (5) depends on the spatial coordinate z.

This gauge choice allows us to deal with a homogeneous problem where the spatial dependence has vanished in Eq. (5). This is a great simplification because allows to use the standard approach and techniques to describe the superconducting state and dynamics. The price to pay for this simplification is to deal with a time-dependent Hamiltonian so that we are forced to solve the time-dependent dynamics. The homogeneity of the system implies that only the $(\mathbf{k}, \uparrow)$ and $(-\mathbf{k}, \downarrow)$ are coupled, consistently simplifying the theoretical analysis.

We can collect the terms in Eq. (5) separating the $\mathbf{k}$ and the $-\mathbf{k}$ contributions. By using the state $\mathbf{\Phi} = \{a_{\mathbf{k}\uparrow}, a^\dagger_{-\mathbf{k}\downarrow}\}$, the relation $h_{-\mathbf{k}_-} = h_{\mathbf{k}_+}$ and the anti-commutation rules for fermionic operators $a^\dagger_{\mathbf{k}\alpha}$ and $a_{\mathbf{k}\alpha}$, we can rewrite Eq. (5) in matrix form as

$$H_{eff} = 2\sum_{\mathbf{k}} \begin{pmatrix} \xi_k & -\Delta \\ -\Delta^* & -\xi_k \end{pmatrix} = 2\sum_{\mathbf{k}} \mathbf{B}_k \cdot \mathbf{\Sigma}_k = 2\sum_{\mathbf{k}} \mathcal{H}_k \tag{10}$$

where

$$\xi_k = \frac{h_{\mathbf{k}_-} + h_{\mathbf{k}_+}}{2} = \frac{\hbar^2 k^2}{2m} + \frac{e^2 E_f^2 t^2}{2m} - \mu, \tag{11}$$

$\mathbf{B}_k = \{-\mathrm{Re}(\Delta), -\mathrm{Im}(\Delta), \xi_k\}$ is a pseudo-magnetic field and $\mathbf{\Sigma}_k = \{\tau_{x,k}, \tau_{y,k}, \tau_{z,k}\}$. This is nothing but the the Anderson pseudospin approach [53].

2.2. Quasi-particle creation: the Superconductive Schwinger effect

To make the dynamics of the superconductive Schwinger effect evident, it is convenient to work in the basis which diagonalizes (10). Since the operator $\mathcal{H}_k$ has the same form of the standard homogeneous case, it can be analytically diagonalized [10]. Considering the original $\{a_{\mathbf{k}\uparrow}, a^\dagger_{-\mathbf{k}\downarrow}\}$ basis, the eigenvalues are $\pm\epsilon_k = \pm\sqrt{\xi_k^2 + |\Delta|^2}$ and the ground and the excited states are, $|\psi_{k,-}(t)\rangle = \{v_k(t), u_k(t)\}$ and $|\psi_{k,+}(t)\rangle = \{u_k^*(t), -v_k^*(t)\}$, respectively, with

$$\begin{aligned} u_k(t) &= \frac{1}{\sqrt{2}}\sqrt{1 + \frac{\xi_k(t)}{\epsilon_k(t)}} e^{-i\chi(t)/2} \\ v_k(t) &= \frac{1}{\sqrt{2}}\sqrt{1 - \frac{\xi_k(t)}{\epsilon_k(t)}} e^{i\chi(t)/2}. \end{aligned} \tag{12}$$

The diagonalizing operator $\mathcal{U}_k$ ($\mathcal{U}_k^\dagger \mathcal{H}_k \mathcal{U}_k = \mathcal{H}_{D,k}$) is time dependent, therefore the dynamics is determined by the following Schroedinger equation

$$i\hbar\partial_t \left|\psi_k(z)\right\rangle = \left(\mathcal{H}_{D,k} - i\hbar\, \mathcal{U}_k^\dagger \partial_t \mathcal{U}_k\right) \left|\psi_k(z)\right\rangle. \tag{13}$$

Notice that Eq. (13) depends on z. Thus, it gives us the dynamics of the k-th mode in position z.

2.2.1. Double excitations The unitary operators $\mathcal{U}_k(t)$ and $\mathcal{U}_k^\dagger(t)$ can be written as

$$\begin{aligned} \mathcal{U}_k &= \begin{pmatrix} u_k^* & v_k \\ -v_k^* & u_k \end{pmatrix} \\ \mathcal{U}_k^\dagger &= \begin{pmatrix} u_k & -v_k \\ v_k^* & u_k^* \end{pmatrix} \end{aligned} \tag{14}$$

with u_k and v_k as in Eq. (12). This leads to the transformation [10]

$$\begin{aligned} \gamma_{\mathbf{k}\uparrow} &= u_k a_{\mathbf{k}\uparrow} - v_k a^\dagger_{-\mathbf{k}\downarrow} \\ \gamma^\dagger_{-\mathbf{k}\downarrow} &= v_k^* a_{\mathbf{k}\uparrow} + u_k^* a^\dagger_{-\mathbf{k}\downarrow} \\ \gamma^\dagger_{\mathbf{k}\uparrow} &= u_k^* a^\dagger_{\mathbf{k}\uparrow} - v_k^* a_{-\mathbf{k}\downarrow} \\ \gamma_{-\mathbf{k}\downarrow} &= v_k a^\dagger_{\mathbf{k}\uparrow} + u_k a_{-\mathbf{k}\downarrow}. \end{aligned} \tag{15}$$

These are the creation-annihilation operators for a quasiparticle that is a superposition of electron and hole [10].

In this representation the diagonal element of $\mathcal{H}_{D,k}$ are associated to the $\gamma^\dagger_{\mathbf{k}\uparrow}\gamma_{\mathbf{k}\uparrow}$ and $\gamma^\dagger_{-\mathbf{k}\downarrow}\gamma_{-\mathbf{k}\downarrow}$. On the contrary, the $\mathcal{U}_k^\dagger\partial_t\mathcal{U}_k$ off-diagonal terms are associated to $\gamma^\dagger_{\mathbf{k}\uparrow}\gamma^\dagger_{-\mathbf{k}\downarrow}$ and $\gamma_{\mathbf{k}\uparrow}\gamma_{-\mathbf{k}\downarrow}$ and, therefore, create or annihilate simultaneously *two quasiparticles* with $(\mathbf{k},\uparrow)$ and $(-\mathbf{k},\downarrow)$. These excitations must be distinguished by the conventional "Bogoliubov quasiparticles" discussed in literature [10] that are related to the destruction of a Cooper pair.

Using the Anderson pseudo-spin formalism is easy to understand the nature of the excited state $|\psi_{k,+}\rangle$. The pairing potential is defined as $\Delta = \sum_k \Delta_k$ with $\Delta_k = V\langle a_{\mathbf{k}\uparrow}a_{-\mathbf{k}\downarrow}\rangle$. For the ground state $|\psi_{k,-}\rangle$, we obtain $\Delta_k = Vu_kv_k^*$ as expected [10]. For the excited state, we have $\Delta_k = -Vu_k(t)v_k^*(t)$ [12]. This can be seen as an additional phase factor $e^{i\pi}$ or, alternatively, a π shift in the superconducting phase associated to Δ_k due to the ground-excited transition.

We conclude that the excited k states preserve the superconductive feature. While the single excitation states (Bogoliubov quasiparticles) are associated to a vanishing coherence factor, i.e., $\langle a_{\mathbf{k}\uparrow}a_{-\mathbf{k}\downarrow}\rangle = 0$, the double excitation states $|\psi_{k,+}\rangle$ are associated to the same coherent factor with a minus sign. This means that a fully excited state, i.e., with all the k modes excited, would have the same pairing potential and the same gap. This implies that the excited state is still superconducting. This fact crucially differentiate the dynamics of the Schwinger-like excitations generated by the external electric field from the thermal quasiparticle excitations. In fact, contrary to the thermal excitations which have vanishing coherence factor, the state generated by the SSE, i.e., the superposition of ground and excited state, is still superconductive. But since the dynamics of the k modes is different, they accumulate a different phase factors. The coherence factor Δ_k is in general a complex number with a time dependent phase. The different phases can generate "interference effects" in the sum $\Delta = \sum_k \Delta_k$ effectively leading to a suppression of the pairing potential and the superconductivity as shown in Fig. 2b.

2.3. Numerical simulations and results

The pairing potential, $\Delta = \sum_k \Delta_k$, is calculated self-consistently during the dynamics. In the numerical simulations, we set $\mu = 1$ eV and the initial pairing potential to $\Delta_0 = 100$ μeV [8]. Moreover we assumed the working temperature to be much smaller than superconducting critical temperature T_C, eventually neglecting thermal excitations. For later convenience, we introduce two reference scales: a time scale $t_{sc} = \hbar/\mu$ and a characteristic electric field $E_C = 5 \times 10^8$ V/m.

We suppose that a constant electric field is applied at time $t_{in} = 0$, and the dynamical transients are negligible. The numerical simulations are performed in a finite time interval

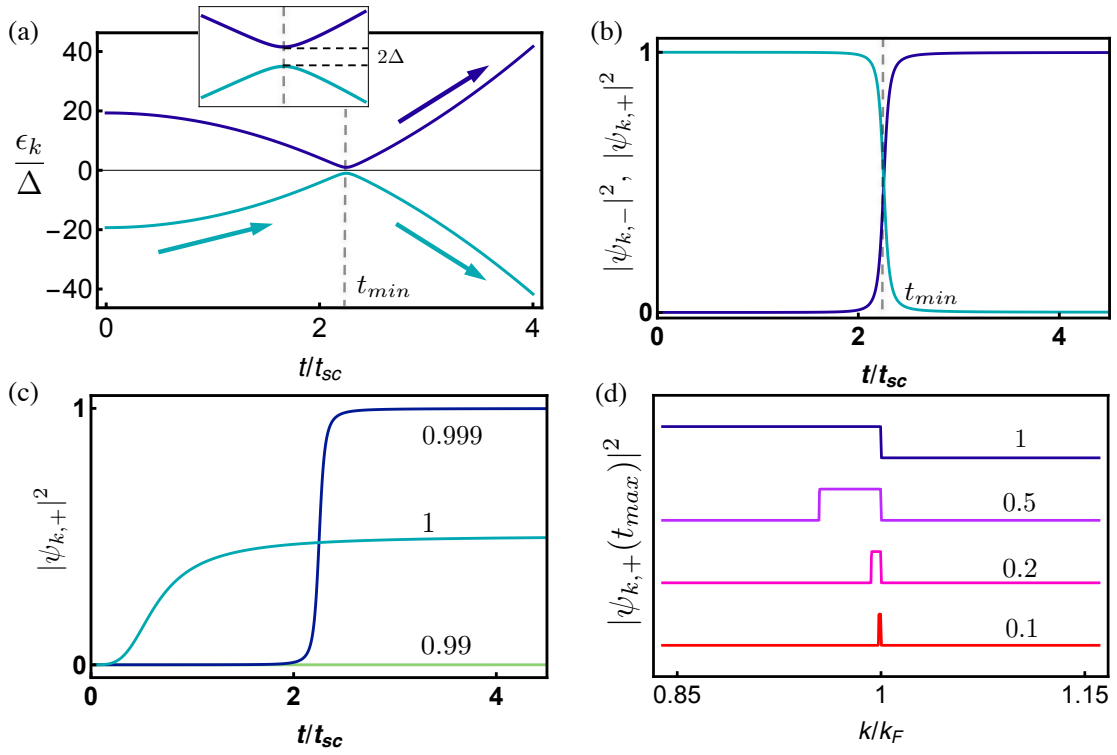

Figure 1. Figure from [38]. (a) Spectrum of the superconductor as a function of time t .The inset shows a zoom of the minimal gap region at $t = t_{min}$. (b) Ground (cyan) and excited state (blue) populations as a function of time. (c) Excited state population as a function of time for $k/k_F = 0.99,\ 0.999$ and 1. In the panels (a) and (b) numerical simulations are performed setting $k/k_F = 0.999$ and in (a), (b) and (c) setting $E_f/E_C = 0.2$. (d) Excited state final population (at $t = t_{max}$) calculated as a function of k/k_F for selected electric fields values, $E_f/E_C = 0.1, 0.2, 0.5, 1$. The curves are shifted for presentation purpose. Simulations are performed setting $\mu = 1$ eV, $\Delta = 100$ μeV and $L = 2$ nm and $z/L = 0.5$.

$0 < t < t_{max}$, where $t_{max} = mL/(\hbar\ k)$ is the time needed for a particle of mass m and momentum k to move from one side to the opposite of a sample of thickness L. This sets the time scale for the numerical simulations. In the latter, we set $L = 2$ nm, so that we can assume a complete penetration of the electric field [54].

The spectrum of the Hamiltonian (10) as a function of time is plotted in Fig. 1(a). The minimum gap 2Δ is reached when the kinetic energy ξ_k in Eq. (5) vanishes, namely for

$$t_{min} = \frac{\sqrt{2\mu m}\sqrt{1-(k/k_F)^2}}{eE_f}. \tag{16}$$

The dynamics of the populations of the ground and excited state $|\psi_{k,-}|^2$ and $|\psi_{k,+}|^2$ is shown in Fig. 1(b) for a fixed k/k_F and E_f/E_C, and presents a clear signature of the SSE. The k-th mode undergoes a sudden transition to the excited state close to the minimal energy gap. This corresponds to the superconducting Schwinger effect, and to the creation of *two* excited quasiparticles, as discussed above.

The dynamics changes considerably for different initial particle momenta, as shown in Fig. 1(c). Away from the Fermi momentum, there is no quasi-particle excitation but moving closer

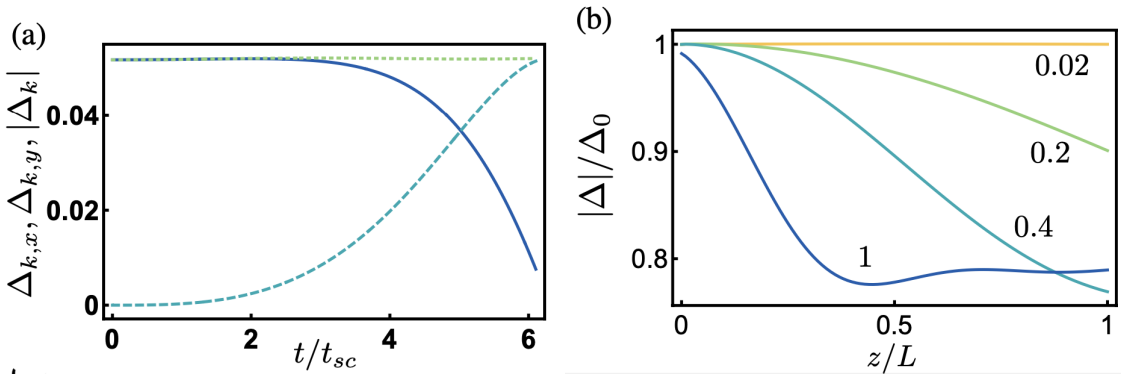

Figure 2. Figure from [38]. (a) Time evolution of $\Delta_{k,x}$ (solid blue), $\Delta_{k,y}$ (dashed cyan) and $|\Delta_k|$ (dotted green) for $k/k_F = 0.999$ and $E_f/E_C = 1$. (b) The normalized order parameter $|\Delta|/\Delta_0$ as a function of z/L, and for different electric fields $E_f/E_C = 0.02, 0.2, 0.4, 1$.

to k_F the system is completely excited. In a small window very close to k_F the system is only partially excited.

A more complete picture can be inferred from Fig. 1(d) where the final population of the excited state $|\psi_{k,+}(t_{max})|^2$ is shown as a function of the momentum for different normalized electric fields E_f/E_C. For small electric field ($E_f/E_C = 0.1$), only a small fraction of the particles around k_F are excited. By increasing the electric field strength, the excited population fraction increases up to a complete excitation for any $k \leq k_F$ and $E_f/E_C = 1$. These results suggest that the electric field at which the excitations are produced is indeed close to E_C and is remarkably similar to the one used in several recent experiments [8, 16, 15, 17, 18, 19, 20, 21, 23, 55, 56, 57, 58].

The values of the critical field can be understood treating the SSE as a Landau-Zener transition [59]. Imposing the condition that the minimal energy gap is reached later than t_{max}, i.e., $t_{min} \leq t_{max}$, the electric field needed to produce the excitations: is $E_f/E_C = (2\mu)/(eE_CL)$. For $L = 2$ nm, we obtain $E_f = 2E_C$, namely close to E_C, as discussed before.

Turning to the superconductive gap Δ, our numerical analysis shows how the coexistence of the ground state together with the double excited state discussed in the previous section creates decoherence, eventually suppressing the gap. In the Anderson pseudo-spin formalism, the order parameter for the k-th mode is $\Delta_k = \Delta_{k,x} + i\Delta_{k,y} = \langle\tau_{x,\mathbf{k}}\rangle + i\langle\tau_{y,\mathbf{k}}\rangle$, where the average $\langle\rangle$ is calculated with state obtained by the dynamical evolution [53, 60, 61]. The numerical calculation displayed in Fig. 2(a) shows that while $|\Delta_k|$ is constant, $\Delta_{k,x}$ and $\Delta_{k,y}$ change in time signaling an accumulated phase. The pairing potential at $t = t_{max}$ is shown in Fig. 2(b) for different electric field values. As the electric field increases the pairing potential is reduced because of the interference effects. Despite the fact that the environmental effects are not included, this already gives strong indications that the presence of a static electric field drastically weakens superconductivity.

3. Tackling the screening problem: a Ginzburg-Landau approach

In the previous section we have proved that, within the BCS framework, a strong enough electric field can activate Schwinger-like excitations, which eventually destabilize the superconducting vacuum by means of decoherence. The electric field needed to activate this process is remarkably similar to the one needed to suppress superconductivity in the experiments in [8]. The main limitation of this analysis was certainly the neglection of screening effect of the electric field. Or, said otherwise, the results described in the previous section are restricted to a thin portion

of the sample near the boundary, where the electric field can be assumed to be constant and of the same order of the external one. In our analysis we have set the maximum thickness of the sample to be 2 nm. However, the superconductive films analyzed in the experiments [8] are at least on coherence length thick (around 100 nm or more). Dealing with such a thick sample it is unavoidable to take into account screening effect of the electric field. To do so at the level of the BCS equation is a tough task. Yet, some insight can be achieved considering an effective Ginzburg-Landau model. The goal of this section is to prove that if one includes in the Ginzburg-Landau functional terms proportional to the electric field which are not typically considered in the usual analysis, it is possible for a suitably strong electric field to suppress superconductivity.

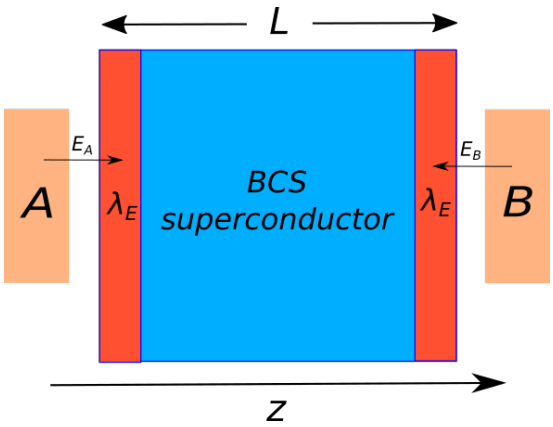

Figure 3. Figure from [39]. Section of the setup. The superconductive film is extended in the x and y direction and has thickness L along the z direction. The electric field E_z pointing along the direction of the small black arrows is applied to both sides of the film, by means of two charge distributions A and B, taken to be equal. The penetration length is $\lambda_E \simeq 1$ nm.

In order to do this, we will analyze the setup depicted in Figure 3, a superconductive thin film extended in the x and y directions and with thickness L in the z direction. The electric field is applied along the z direction by means of two charge distributions (A and B in Figure 3) placed in the vicinity of the surfaces of the film. This setup is similar to the one realized in the experiments [29]. In what follows the charges A and B are assumed to be equal. This implies that the direction of the electric field is reversed as we cross the middle of the channel at $z = L/2$ (see Fig. 3). The physical results do not depend appreciably on the sign of the charges and on such a symmetric configuration [29] whose purpose is simplifying numerical computations. We include screening effects in our model by assuming that they are set at the level of the normal metal phase. Due to the reduced thickness of the sample we assume the electric field generated by the charges A and B inside the material to be along the z-direction. Hence we fix the applied electric field $\vec{E}$ to be non-dynamical with a decreasing exponential profile at the ends ($z = 0$ and $z = L$) of the film i.e.

$$\vec{E} = -\partial_z \varphi(z)\hat{z} = 2E_0 e^{-\frac{L}{2\lambda_E}} \sinh\left(\frac{\frac{L}{2} - z}{\lambda_E}\right)\hat{z}\,. \tag{17}$$

We take the penetration length, λ_E, to be $\simeq 1$ nm which is compatible with normal metals [62]. Note that the above formula for the electric field implies that the sample is charged, this however is an artifact of the simple screening model, as we are considering a charged-neutral film. Since the film is much larger than the penetration length, the spurious charge distribution in the bulk

that would make it overall neutral will give rise to negligible effects and we consequently ignore it.

3.1. The model

Now consider the mean field description [11, 63] of this configuration. We use the usual complex scalar superconductive order parameter written in polar form $\Psi(\vec{r}) = \Delta(\vec{r}) \exp[i\theta(\vec{r})]$ where $\Delta(\vec{r})$ and $\theta(\vec{r})$ are the amplitude and the phase of the order parameter, respectively. Having fixed the electric field profile, we focus on time independent configurations. Consequently, the resulting time-independent GL free energy is

$$F = \int d^3r \left\{ \frac{\hbar^2}{2m} \|\vec{\partial}\Delta\|^2 + \frac{\hbar^2}{2m}\Delta^2 \|\vec{\partial}\theta\|^2 + \left(\frac{\alpha_2}{2!} + q\varphi\right)\Delta^2 + \frac{\alpha_4}{4!}\Delta^4 + \frac{\epsilon[\Delta]}{2}\left(\frac{d\varphi}{dz}\right)^2 \right\} \tag{18}$$

where m, q are the mass and charge of the Cooper pair respectively, $\varphi(z)$ is defined in (17) and $\|\vec{x}\|$ is the vector norm of $\vec{x}$.

Our free energy (18) differs from the usual GL free energy [11, 63] by allowing the electric permittivity to depend on the condensate density Δ. We will assume the following functional dependence on Δ:

$$\epsilon[\Delta] = \epsilon_0 \left(1 + \beta_1 \Delta^2 + \beta_2 \Delta^4 + \ldots\right) , \tag{19}$$

where β_1 and β_2 are phenomenological parameters. These additional couplings respect all the symmetries of the system and are at most quartic in the gap and quadratic in derivatives. It is consequently natural to include them within a GL functional approach. The conditions for the expansion (19) to be consistent are $\beta_1\Delta_0^2 \ll 1$, $\beta_2\Delta_0^4 \ll 1$ where $\Delta_0^2 = -3\alpha_2/2\alpha_4$ is a homogeneous condensate density in absence of an electric field.

Analogous terms in the electric permittivity (19) already occur in the BCS context [64] due to perturbative loop corrections around the (constant, spatially independent) BCS ground state. The same perturbative approach has been followed in [65]. We however consider a new, inhomogeneous (coordinate dependent) ground state generated by solving the full GL equations in the presence of an external electric field. Moreover, we promote the corrections to the permittivity found in [64] to be interactions of the bare GL functional (18). This corresponds to finding a complete non-perturbative solution to the Ginzburg Landau equation including interactions between the order parameter and the electric field. Qualitatively our results agree with [64, 65] when the applied electric field is sufficiently small. Moreover, in what follows we will prove that even parametrically small coupling constants β_1 and β_2 have dramatic consequences on the order parameter Δ, when the external electric field cannot be treated as a perturbative correction (as in [64]).

3.2. Driving the phase transition

The minimal energy solutions for the equations of motion resulting from (18) have constant phase θ as can be seen by examining the equation of motion,

$$\vec{\partial} \cdot \left(\Delta^2 \vec{\partial}\theta\right) = 0 ,$$

and minimizing the contribution of the second integrand in (18) to the free energy. The equation for Δ then reduces to

$$\frac{\hbar^2}{m}\vec{\partial}^2\Delta - \left(\alpha_2 + 2q\varphi + \epsilon_0\beta_1\left(\frac{d\varphi}{dz}\right)^2\right)\Delta - \left(\frac{\alpha_4}{3!} + 2\epsilon_0\beta_2\left(\frac{d\varphi}{dz}\right)^2\right)\Delta^3 = 0 . \tag{20}$$

This equation has to be solved imposing the usual boundary conditions at the edges of the material $\Delta'(0) = \Delta'(L) = 0$ [63]. The z-dependent profile for the electric field in (17) makes the solution of (20) depend on z as well. Since we are interested in global observables (e.g. the critical current of the full thin film) the relevant quantity will be the averaged gap $\Delta_{\text{av.}} = \frac{1}{L}\int_0^L dz\ \Delta(z)$. We refer to the Appendix for technical details about the numerical solution of equation (20).

To have a direct comparison with the experiments, we consider the devices used in [8]. We take $T_{\text{c}} \simeq 410$ mK, London penetration length $\lambda_L \simeq 900$ nm and the coherence length $\xi_0 \simeq 100$ nm. We also assume the usual GL temperature scalings for the relevant parameters, so that $\alpha_2 = -\mathcal{K}(1 - T/T_{\text{c}})$ with $\mathcal{K} = 6.104 \times 10^{-25}$ kg m^2 s^{-2} and $\alpha_4 = 6.356 \times 10^{-50}$ kg m^5 s^{-2}.

The parameters β_1 and β_2 in (19) are phenomenological, and, in order to fix them, we rely on experimental observations [8]. To qualitatively understand their effect, suppose we can ignore the kinetic energy. This is certainly true in films thin enough such that the electric field penetrates deeper in the bulk. In this case one can define new effective GL parameters $\tilde{\alpha_2}$ and $\tilde{\alpha_4}$ averaged over the system: $\tilde{\alpha}_2 = \alpha_2 + 2q\varphi_{\text{av.}} + \epsilon_0\beta_1 E^2_{\text{av.}}$ and $\tilde{\alpha}_4 = \alpha_4 + 12\epsilon_0\beta_2 E^2_{\text{av.}}$, where $\varphi_{\text{av.}}$ and $E_{\text{av.}}$ are the space averages of the scalar potential and the electric field respectively. As in the standard GL model, the phase is consequently determined by the sign of $\tilde{\alpha}_2$ (negative for superconducting, positive for metal) [11]. If $\beta_1 > 0$ is chosen carefully, since $\alpha_2 < 0$, we can set $\tilde{\alpha}_2 = 0$ for some critical averaged electric field $E^{\text{c}}_{\text{av.}}$, which determines the critical point. Similarly, $\tilde{\alpha}_4$ affects the form of the potential energy (e.g. position of minima) and, therefore, the dependence of Δ on E_z. It does not, however, affect the value of $E^{\text{c}}_{\text{av.}}$.

Focusing on samples with thickness of the order of the coherence length ($L \simeq \xi_0$), from the experimental data [8], it turns out that β_1 has a linear dependence on T,

$$\beta_1 = \left[A + B\left(1 - \frac{T}{T_{\text{c}}}\right)\right]\ \text{m}^3\ , \tag{21}$$

with $A = 1.208 \times 10^{-30}$ and $B = 5.947 \times 10^{-28}$. The presence of the positive constant A ensures that in the limit of $T \to T_{\text{c}}$, β_1 remains positive. This means that when the superconductor is in the normal phase but close to T_{c}, the electric field cannot induce a phase transition to the superconducting state. With this information (21) we can estimate the correction to the critical temperature due to the β_1 coupling. In particular, $\tilde{\alpha}_2(0) = (1 - T/T_{\text{c}})(-\mathcal{K} + \epsilon_0 B(E^{\text{c}}_{\text{av.}})^2) + \epsilon_0 A(E^{\text{c}}_{\text{av.}})^2$. Assuming $E^{\text{c}}_{\text{av.}} \sim 10^8$ V/m as in [8], we can solve the above equation for $\tilde{\alpha}_2 = 0$, obtaining a new critical temperature $T_{\text{c},new}$ and a variation $\Delta T_{\text{c}} = T_{\text{c},new} - T_{\text{c}} \propto 3 - 4$ mK. This is a rough estimate but is compatible with the full numerical simulations and the absence of variation of T_{c} observed in the experiments [27].

Finally, the second parameter β_2, is obtained as the best fit of experimental data. As it is a best fit parameter and the temperature range of the experimental data is small, it is difficult to extract a precise temperature dependence. Nevertheless we find that this parameter has a mild temperature dependence, with $-4 \times 10^{-54}\ \text{m}^6 \lesssim \beta_2 \lesssim -6 \times 10^{-54}\ \text{m}^6$ for the range of temperatures examined.

We are now in position to discuss the numerical results derived from the solution of the full GL equation (20), which are presented in Fig. 4. Fig. 4 a) displays the critical current of the wire, i.e. the maximal current that the superconductor can sustain [11], $\mathcal{I}_{\text{c}}$ against the applied electric field at the material boundaries, E_0, for various temperatures. In GL theory, $\mathcal{I}_{\text{c}} \propto \Delta^3$; in our inhomogeneous situation, we take $\mathcal{I}_{\text{c}} \propto (\Delta_{\text{av.}})^3$ [1]. As displayed, the presence of a strong electric field weakens superconductivity and eventually leads to a vanishing $\mathcal{I}_{\text{c}}$ which corresponds to a superconducting to normal phase transition (i.e. $\Delta(z) \to 0$). The numerical simulations reproduce the qualitative behavior of the experiments [8] at low temperatures. This should be

[1] $(\Delta_{\text{av.}})^3$ is almost equivalent to $(\Delta^3)_{\text{av.}}$, as the profiles are weakly dependent on z.

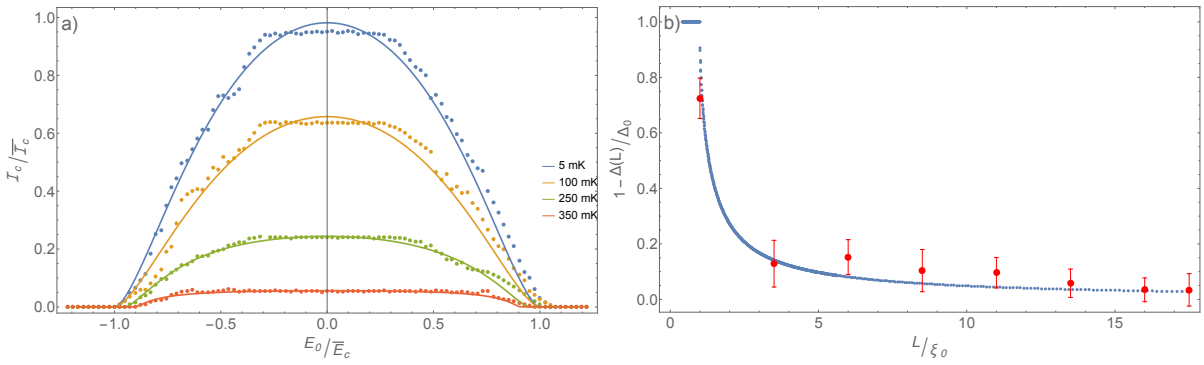

Figure 4. Figure from [39]. **a)**: Numerical computation of the averaged critical current $\mathcal{I}_c$ normalized against its values at $T = 5$ mK, $\bar{\mathcal{I}}_c$, as a function of the applied electric field E_0 (see (17)) normalized against the 5 mK critical electric field $\bar{E}_c$. The curves are the numerical simulations and the dots are the experimental data from [8]. The values of $\bar{\mathcal{I}}_c$ at different temperatures are taken from the experiments. The parameters β_1 and β_2 are fixed as discussed in the text. **b)**: The suppression of the electric field effect as a function of the thickness of the film L for $T = 5$ mK and $E = \bar{E}_c$. The red dots are the experimental data from [8].

expected, since the GL approach to superconductivity is expected to be accurate for $T \lesssim T_c$. For larger temperatures, our GL model is only expected to reproduce the qualitative features of superconductive transport, as seen in Fig. 4 a).

From the numerical data for $\mathcal{I}_c$ we observe a small asymmetry in the critical electric field between positive and negative choices for the electrodes. This is evident from the equation of motion for the gap (20) as the chemical potential term, $q\varphi$, is not symmetric under $E_0 \to -E_0$. Such an asymmetry also seems to be present in the experimental data, but the effect is significantly stronger than what we predict. It remains to be demonstrated experimentally whether this is a real effect, as this would point to additional terms missing from our modified GL free energy (18).

An important feature of the experimental data which has not yet been explained in the literature is the emergence of the coherence length scale in the dependence of the SFE on film thickness. To examine this issue, we set $T = 5$ mK and $E_0 = \bar{E}_c \simeq 10^8$ V m^{-1} and consider films with different thicknesses L. Plots for other temperatures are qualitatively similar. The numerical results are sketched in Figure 4 b). For $L \lesssim \xi_0$ the electric field causes a complete phase transition to the metallic phase. As $L > \xi_0$ is increased, one finds that the same external electric field does not completely suppress the gap. The effect becomes completely irrelevant if the sample is thicker than $7 - 8$ coherence lengths. This behavior matches the experimental observations [8, 16, 15] (shown with the red dots in the figure).

This latter observation strongly supports the idea that the SFE emerges from an interplay between the small electric field penetration length λ_E and the much larger superconducting coherence length ξ_0. This has an interesting interpretation in terms of the renormalization group. The naive scaling dimension of the couplings β_1 and β_2 shows that these terms are marginal in $d = 2$ dimensions and irrelevant for $d > 2$. When $L \simeq \xi_0$, and the material is effectively two dimensional, there can be a phase transition as the β-corrections are important for defining the low energy behavior of the Effective Field Theory (EFT). This numerical and theoretical analysis also explains why these kinds of phase transition have never been seen in extended three dimensional samples.

4. Conclusions

In this paper we have reviewed the results of [38, 39], in which the effects of a strong electric field in a superconductor are analyzed.

From the microscopic side, in [38] the electric field is assumed to completely penetrates the sample and the BCS equations are eventually solved numerically. Consequently, the analysis is restricted to very thin films (a few nanometers thick) or, said otherwise, to a very narrow portion near the boundary of a bulk material. This is due to the fact that screening effects in superconductors should be comparable to the ones occurring in a normal metal, and the electric field should not penetrate inside the material more than 2-3 nm. In any case, the numerical analysis of [38] shows that a suitably strong electric field can activate the creation of a very peculiar kind of excitations, in which two quasi-particles are created from the BCS vacuum. This mechanism has a strong analogy with the QED Schwinger effect, so that this effect has been named the Superconductive Schwinger Effect. The excitations created in this manner are still in the superconductive space. This means that the expectation value of the superconductive order parameter on this excited state has the same absolute value of the ground-state one, but with a shift of the phase by a factor π. This implies that the coexistence of the ground state together with this Schwinger-like excited state can create decoherence, eventually suppressing superconductivity. Remarkably, the order of magnitude of the electric field needed to activate the Superconductive Schwinger effect is exactly the same as the one needed in the experiments of [8] to suppress the supercurrent.

However, to make contact with the experiments and to propose the Superconductive Schwinger Effect as the microscopic origin of the phenomenon measured in [8], screening effects must be taken into account. To include them in the BCS framework is a tough task, and in [39] the effective Ginzburg Landau approach has been preferred instead. In this paper, additional higher derivatives terms proportional to the electric field have been added to the conventional textbook Ginzburg-Landau free energy [11]. In an effective field theory approach, these additional terms, being higher derivatives corrections, can be typically neglected, except when the electric field becomes parametrically large. The screening effects have been included in the model by considering a fixed exponentially decaying profile for the electric field, with a penetration length of 1 nm, the same of a normal metal. The model shows that a strong enough electric field can destroy superconductivity even considering screening effects. Various observables have been computed, finding a remarkable agreement with the experiments in [8]. The main problem of this analysis is that the additional coupling constants considered in the Ginzburg-Landau theory have been fixed phenomenological, by imposing that the electric field needed to suppress superconductivity is the same found in the experiments [8]. Consequently, the model proves that the phenomenon measured in [8] can be explained as a phase transition from a superconductor to a normal metal driven by the electric field, but does not provide a microscopic origin for the additional coupling constants considered in the analysis.

The next step in the program would be to make contact between the microscopic boundary analysis of [38] and the effective field theory analysis of [39]. A first step in this direction should be to include an external electric field in the Gork'ov equations [66], and to solve them numerically. This will give us the full set of correlators in the presence of an external electric field. In particular, this analysis will make it possible to compute the density of states of the system, and to design new obersvables which can be measured to further test the hypothesis of [38]. To do so however, a stationary states must be found, and consequently dissipation effects must be included in the Gork'ov equations.

References

[1] Ashcroft N W and Mermin N D 1976 *Solid State Physics* (Holt-Saunders)

[2] Castro Neto A H, Guinea F, Peres N M R, Novoselov K S and Geim A K 2009 *Rev. Mod. Phys.* **81**(1) 109–162
[3] Armitage N P, Mele E J and Vishwanath A 2018 *Rev. Mod. Phys.* **90**(1) 015001
[4] Isobe H and Nagaosa N 2012 *Phys. Rev. B* **86**(16) 165127
[5] Yang B J, Moon E G, Isobe H and Nagaosa N 2014 *Nature Physics* **10** 774–778 ISSN 1745-2481
[6] Landsteiner K 2014 *Phys. Rev. B* **89**(7) 075124
[7] Allor D, Cohen T D and McGady D A 2008 *Physical Review D* **78** ISSN 1550-2368
[8] De Simoni G, Paolucci F, Solinas P, Strambini E and Giazotto F 2018 *Nature Nanotechnology* **13** 802–805 (*Preprint* 1710.02400)
[9] Bardeen J, Cooper L N and Schrieffer J R 1957 *Phys. Rev.* **108**(5) 1175–1204
[10] De Gennes P G 1999 *Superconductivity of Metals and Alloys* Advanced book classics (Cambridge, MA: Perseus)
[11] Tinkham M 2004 *Introduction to Superconductivity* Dover Books on Physics Series (Dover Publications) ISBN 9780486134727
[12] Leggett A 2006 *Quantum Liquids: Bose condensation and Cooper pairing in condensed-matter systems* Oxford Graduate Texts (OUP Oxford) ISBN 9780198526438
[13] Kopnin N 2009 *Theory of Nonequilibrium Superconductivity* International Series of Monographs on Physics (OUP Oxford) ISBN 9780199566426
[14] Amoretti A, Braggio A, Caruso G, Maggiore N and Magnoli N 2014 *JHEP* **04** 142
[15] Ritter M F, Fuhrer A, Haxell D Z, Hart S, Gumann P, Riel H and Nichele F 2021 *Nature Communications* **12** ISSN 2041-1723
[16] Alegria L D, Bøttcher C G L, Saydjari A K, Pierce A T, Lee S H, Harvey S P, Vool U and Yacoby A 2021 *Nature Nanotechnology* **16** 404–408 ISSN 1748-3395
[17] Golokolenov I, Guthrie A, Kafanov S, Pashkin Y A and Tsepelin V 2021 *Nature Communications* **12** ISSN 2041-1723
[18] Orús P, Fomin V, De Teresa J and Córdoba R 2021 *Sci. Rep.* **11**
[19] Basset J, Stanisavljević O, Kuzmanović M, Gabelli J, Quay C H L, Estève J and Aprili M 2021 *Phys. Rev. Research* **3**(4) 043169
[20] Ritter M F, Crescini N, Haxell D Z, Hinderling M, Riel H, Bruder C, Fuhrer A and Nichele F 2021 *Nature Electronics* **5** 71–77
[21] Elalaily T, Kürtössy O, Scherübl Z, Berke M, Fülöp G, Lukács I E, Kanne T, Nygård J, Watanabe K, Taniguchi T, Makk P and Csonka S 2021 *Nano Letters* **21** 9684–9690
[22] Amoretti A, Meinero M, Brattan D K, Caglieris F, Giannini E, Affronte M, Hess C, Buechner B, Magnoli N and Putti M 2020 *Phys. Rev. Res.* **2** 023387 (*Preprint* 1909.07991)
[23] Amoretti A, Blasi A, Caruso G, Maggiore N and Magnoli N 2013 *Eur. Phys. J. C* **73** 2461 (*Preprint* 1301.3688)
[24] Paolucci F, Crisá F, De Simoni G, Bours L, Puglia C, Strambini E, Roddaro S and Giazotto F 2021 *Nano Letters* **21** 10309–10314
[25] Mercaldo M T, Solinas P, Giazotto F and Cuoco M 2020 *Phys. Rev. Applied* **14**(3) 034041
[26] Chirolli L, Cea T and Giazotto F 2021 *Phys. Rev. Research* **3**(2) 023135
[27] Paolucci F, De Simoni G, Strambini E, Solinas P and Giazotto F 2018 *Nano Letters* **18** 4195–4199 ISSN 1530-6992
[28] Paolucci F, De Simoni G, Solinas P, Strambini E, Puglia C, Ligato N and Giazotto F 2019 *AVS Quantum Science* **1** 016501 ISSN 2639-0213
[29] Paolucci F, De Simoni G, Solinas P, Strambini E, Ligato N, Virtanen P, Braggio A and Giazotto F 2019 *Physical Review Applied* **11** ISSN 2331-7019
[30] Paolucci F, Vischi F, De Simoni G, Guarcello C, Solinas P and Giazotto F 2019 *Nano Letters* **19** 6263–6269 ISSN 1530-6992
[31] Amoretti A, Brattan D K, Magnoli N and Scanavino M 2020 *JHEP* **08** 097 (*Preprint* 2005.09662)
[32] Amoretti A, Arean D, Brattan D K and Magnoli N 2021 *JHEP* **05** 027 (*Preprint* 2101.05343)
[33] Rocci M, De Simoni G, Puglia C, Esposti D D, Strambini E, Zannier V, Sorba L and Giazotto F 2020 *ACS Nano* **14** 12621–12628 ISSN 1936-086X
[34] Bours L, Mercaldo M T, Cuoco M, Strambini E and Giazotto F 2020 *Phys. Rev. Research* **2**(3) 033353
[35] Puglia C, De Simoni G, Ligato N and Giazotto F 2020 *Applied Physics Letters* **116** 252601
[36] De Simoni G, Puglia C and Giazotto F 2020 *Applied Physics Letters* **116** 242601
[37] Rocci M, Suri D, Kamra A, Vilela G, Takamura Y, Nemes N M, Martinez J L, Hernandez M G and Moodera J S 2020 *Nano Letters* **21** 216–221 ISSN 1530-6992
[38] Solinas P, Amoretti A and Giazotto F 2021 *Phys. Rev. Lett.* **126**(11) 117001
[39] Amoretti A, Brattan D K, Magnoli N, Martinoia L, Matthaiakakis I and Solinas P 2022 *Phys. Rev. Res.* **4**

033211 (*Preprint* 2202.00687)
[40] Ruffini R, Vereshchagin G and Xue S S 2010 *Physics Reports* **487** 1–140 ISSN 0370-1573
[41] Dunne G V 2012 *Int. J. Mod. Phys. Conf. Ser.* **14** 42–56 (*Preprint* 1202.1557)
[42] Gelis F and Tanji N 2016 *Progress in Particle and Nuclear Physics* **87** 1–49 ISSN 0146-6410
[43] Sauter F 1931 *Z. Phys.* **69** 742–764
[44] Heisenberg W and Euler H 1936 *Z. Phys.* **98** 714–732 (*Preprint* physics/0605038)
[45] Schwinger J 1951 *Phys. Rev.* **82**(5) 664–679
[46] Zener C 1932 *Proc. Roy. Soc. Lond. A* **137** 696–702
[47] Lacki J, Ruegg H and Wanders G (eds) 2009 *Theorie der unelastischen Stösse zwischen Atomen* (Basel: Birkhäuser Basel) pp 117–171
[48] Majorana E 1932 *Il Nuovo Cimento (1924-1942)* **9**(5) 43–50
[49] Nambu Y and Jona-Lasinio G 1961 *Phys. Rev.* **122** 345–358
[50] Nambu Y and Jona-Lasinio G 1961 *Phys. Rev.* **124** 246–254
[51] Nambu Y 1960 *Phys. Rev.* **117**(3) 648–663
[52] Aitchison I J R and Hey A J G 2012 *Gauge theories in particle physics: A practical introduction. Vol. 2: Non-Abelian gauge theories: QCD and the electroweak theory* (CRC Press) ISBN 978-1-4665-1307-5
[53] Anderson P W 1958 *Phys. Rev.* **112**(6) 1900–1916
[54] Piatti E, Daghero D, Ummarino G A, Laviano F, Nair J R, Cristiano R, Casaburi A, Portesi C, Sola A and Gonnelli R S 2017 *Phys. Rev. B* **95**(14) 140501
[55] Amoretti A, Braggio A, Maggiore N, Magnoli N and Musso D 2014 *JHEP* **09** 160 (*Preprint* 1406.4134)
[56] Amoretti A and Brattan D K 2022 *Mod. Phys. Lett. A* **37** 2230010 (*Preprint* 2209.11589)
[57] Amoretti A, Brattan D K, Martinoia L and Matthaiakakis I 2022 (*Preprint* 2211.05791)
[58] Amoretti A, Brattan D K, Martinoia L and Matthaiakakis I 2022 (*Preprint* 2212.09761)
[59] Cohen T D and McGady D A 2008 *Phys. Rev. D* **78**(3) 036008
[60] Tsuchiya S, Yamamoto D, Yoshii R and Nitta M 2018 *Phys. Rev. B* **98**(9) 094503
[61] Tsuji N and Aoki H 2015 *Phys. Rev. B* **92**(6) 064508
[62] Ashcroft N, W A, Mermin N, Ashcroft W, Mermin D, Mermin N and Company B P 1976 *Solid State Physics* HRW international editions (Holt, Rinehart and Winston) ISBN 9780030839931
[63] Kopnin N and Press O U 2001 *Theory of Nonequilibrium Superconductivity* International Series of Monographs on Physics (Clarendon Press) ISBN 9780198507888
[64] Prange R E 1963 *Phys. Rev.* **129**(6) 2495–2503
[65] Virtanen P, Braggio A and Giazotto F 2019 *Phys. Rev. B* **100**(22) 224506
[66] Gorkov L P 1918 (1959) *Zh. Eksp. Teor. Fiz. [Sov. Phys. JETP 9, 1364(1959)]* **36**